



OPEN ACCESS

EDITED BY

Chad Quarles,
University of Texas MD Anderson Cancer
Center, United States

REVIEWED BY

David A. Hormuth, II,
The University of Texas at Austin,
United States
Ralph Peter Mason,
University of Texas Southwestern Medical
Center, United States

*CORRESPONDENCE

Caterina Brighi
✉ caterina.brighi@sydney.edu.au

RECEIVED 03 October 2023

ACCEPTED 04 December 2023

PUBLISHED 19 December 2023

CITATION

Brighi C, Waddington DEJ, Keall PJ, Booth J, O'Brien K, Silvester S, Parkinson J, Mueller M, Yim J, Bailey DL, Back M and Drummond J (2023) The MANGO study: a prospective investigation of oxygen enhanced and blood-oxygen level dependent MRI as imaging biomarkers of hypoxia in glioblastoma. *Front. Oncol.* 13:1306164. doi: 10.3389/fonc.2023.1306164

COPYRIGHT

© 2023 Brighi, Waddington, Keall, Booth, O'Brien, Silvester, Parkinson, Mueller, Yim, Bailey, Back and Drummond. This is an open-access article distributed under the terms of the [Creative Commons Attribution License \(CC BY\)](https://creativecommons.org/licenses/by/4.0/). The use, distribution or reproduction in other forums is permitted, provided the original author(s) and the copyright owner(s) are credited and that the original publication in this journal is cited, in accordance with accepted academic practice. No use, distribution or reproduction is permitted which does not comply with these terms.

The MANGO study: a prospective investigation of oxygen enhanced and blood-oxygen level dependent MRI as imaging biomarkers of hypoxia in glioblastoma

Caterina Brighi^{1*}, David E. J. Waddington¹, Paul J. Keall¹, Jeremy Booth^{2,3}, Kieran O'Brien⁴, Shona Silvester¹, Jonathon Parkinson^{5,6}, Marco Mueller⁴, Jackie Yim^{2,6,7}, Dale L. Bailey⁸, Michael Back^{2,6} and James Drummond^{2,6,9}

¹Image X Institute, Sydney School of Health Sciences, The University of Sydney, Sydney, NSW, Australia, ²Department of Radiation Oncology, Northern Sydney Cancer Centre, Royal North Shore Hospital, Sydney, NSW, Australia, ³Institute of Medical Physics, School of Physics, The University of Sydney, Sydney, NSW, Australia, ⁴Siemens Healthcare Pty Ltd, Brisbane, QLD, Australia, ⁵Department of Neurosurgery, Royal North Shore Hospital, Sydney, NSW, Australia, ⁶The Brain Cancer Group Sydney, St Leonards, NSW, Australia, ⁷Centre for Health Economics Research and Evaluation, University of Technology Sydney, Sydney, NSW, Australia, ⁸Department of Nuclear Medicine, Royal North Shore Hospital, Sydney, NSW, Australia, ⁹Department of Neuroradiology, Royal North Shore Hospital, Sydney, NSW, Australia

Background: Glioblastoma (GBM) is the most aggressive type of brain cancer, with a 5-year survival rate of ~5% and most tumours recurring locally within months of first-line treatment. Hypoxia is associated with worse clinical outcomes in GBM, as it leads to localized resistance to radiotherapy and subsequent tumour recurrence. Current standard of care treatment does not account for tumour hypoxia, due to the challenges of mapping tumour hypoxia in routine clinical practice. In this clinical study, we aim to investigate the role of oxygen enhanced (OE) and blood-oxygen level dependent (BOLD) MRI as non-invasive imaging biomarkers of hypoxia in GBM, and to evaluate their potential role in dose-painting radiotherapy planning and treatment response assessment.

Methods: The primary endpoint is to evaluate the quantitative and spatial correlation between OE and BOLD MRI measurements and [¹⁸F]MISO values of uptake in the tumour. The secondary endpoints are to evaluate the repeatability of MRI biomarkers of hypoxia in a test-retest study, to estimate the potential clinical benefits of using MRI biomarkers of hypoxia to guide dose-painting radiotherapy, and to evaluate the ability of MRI biomarkers of hypoxia to assess treatment response. Twenty newly diagnosed GBM patients will be enrolled in this study. Patients will undergo standard of care treatment while receiving additional OE/BOLD MRI and [¹⁸F]MISO PET scans at several timepoints during treatment. The ability of OE/BOLD MRI to map hypoxic tumour regions will be evaluated by assessing

spatial and quantitative correlations with areas of hypoxic tumour identified via [¹⁸F]MISO PET imaging.

Discussion: MANGO (Magnetic resonance imaging of hypoxia for radiation treatment guidance in glioblastoma multiforme) is a diagnostic/prognostic study investigating the role of imaging biomarkers of hypoxia in GBM management. The study will generate a large amount of longitudinal multimodal MRI and PET imaging data that could be used to unveil dynamic changes in tumour physiology that currently limit treatment efficacy, thereby providing a means to develop more effective and personalised treatments.

KEYWORDS

glioblastoma, hypoxia imaging, magnetic resonance imaging, radiotherapy, dose painting, treatment response assessment

1 Introduction

Glioblastoma (GBM) is the most aggressive type of brain cancer and carries an extremely poor prognosis, which is reflected in 5-year survival of 5% and an overall median survival time of approximately 17 months following first-line treatment (1). After standard of care treatment, involving maximal safe resection of the bulk tumour mass followed by adjuvant chemoradiation treatment, most tumours recur locally, highlighting the failure of current treatment approaches to sustain local control (2, 3). The large intra- and inter-tumour heterogeneity characterising GBMs and the ability of GBM cells to dynamically adapt during the course of treatment and develop treatment resistance mechanisms are causes of local treatment failure (4). As such, the future of improved treatment outcomes for GBM patients relies on personalised treatment strategies targeting known mechanisms of treatment resistance.

Hypoxia, which is often present in subregions of GBM tumours, is the leading cause of resistance to radiotherapy, is predictive of the local sites of recurrence and is associated with poor clinical outcomes in GBM (5–12). Current standard of care treatment does not account for tumour hypoxia. The ability to image tumour hypoxia at various stages of treatment offers opportunities to personalise and improve treatments for GBM patients (13). For instance, preoperative imaging of tumour hypoxia offers the opportunity for supramarginal resections in surgical planning beyond current neurosurgical standard of care guidelines (14). Identifying hypoxic regions by using specialised imaging potentially allows adaptive radiotherapy treatment planning and delivery strategies to selectively dose escalate to radioresistant tumour regions, thus increasing the likelihood of local control (10, 15). Identifying hypoxic tumour regions harbouring progression at follow up is key to intervening at an

early stage of tumour recurrence and personalising therapy tailored to the tumour response to treatment (16).

Imaging of tumour hypoxia in routine clinical practice is challenging, as it requires [¹⁸F]MISO PET (13, 17), which is not available in most clinical centres (18). MRI, which is the core imaging modality in the management of GBM patients and is available at most clinical sites, offers a more cost effective and accessible means to integrating imaging biomarkers of hypoxia into clinical workflows (19, 20). Additionally, the combination of MRI screening with radiotherapy is becoming more common with the growth in integrated MRI-guided radiotherapy systems (21). In this clinical imaging study, we aim to validate oxygen enhanced (OE) and blood-oxygen level dependent (BOLD) MRI as imaging biomarkers of hypoxia at different stages of GBM treatment, and evaluate potential patients benefits arising from their integration into radiotherapy treatment planning and in treatment response assessment.

Several preclinical studies have already shown the ability of OE/BOLD MRI to identify areas of hypoxic tumour and use this information to improve cancer treatment and response assessment. For instance, Zhou et al. demonstrated that OE/BOLD MRI measurements correlate with levels of [¹⁸F]MISO uptake in hypoxic tumour of a rat prostate cancer model (22), thus showing its potential as an alternative, non-invasive imaging biomarker of hypoxia. White et al. have shown the ability of OE MRI to predict tumour response to radiation treatment in a preclinical model of prostate cancer, thus showing the potential of OE MRI for adaptive radiotherapy treatment strategies (23). This finding was further confirmed by Arai et al., who demonstrated the predictive value of OE MRI in response to radiation treatment in a rat model of prostate cancer (24). The authors additionally showed an improvement in tumour control resulting from the delivery of a

10 Gy boost of radiation dose to hypoxic tumours identified with OE MRI (24). Beeman et al. have demonstrated that OE MRI has the ability to differentiate progressing tumour lesions from radiation necrosis lesions in a preclinical glioma study (25), showing OE MRI potential for improved response assessment applications. Finally, in a recent clinical study Lickliter et al. demonstrated the utility of OE MRI to assess tumour response to the administration of a novel hypoxia modifying agent in combination with standard chemoradiation therapy in GBM patients (26).

Overall, by performing this study, we expect to provide a non-invasive, more effective means to adapt treatment to the individual tumour characteristics of each patient, that can be accessible to many clinical centres worldwide.

2 Methods and analysis

2.1 Study objectives

The study has one primary and four secondary objectives (Figure 1). The primary objective is to evaluate the spatial and quantitative correlations between OE and BOLD MRI measurements of hypoxia and [¹⁸F]MISO values of uptake in the tumour once before patients receive surgery and once prior to commencement of chemoradiation treatment. The secondary objectives are: 1) to evaluate the repeatability of the MRI biomarkers of hypoxia by means of test-retest scans acquired prior to patients commencement of chemoradiation treatment; 2) to develop a framework to integrate image-derived tumour hypoxia information into radiation treatment plans and estimate the potential clinical benefits of this approach compared to conventional radiation treatment; 3) to evaluate the ability of MRI biomarkers of hypoxia to assess tumour response to chemoradiation treatment; 4) to evaluate whether changes in the MRI biomarker of hypoxia observed during chemoradiation

treatment are predictive of patient overall survival. Secondary objectives 3 and 4 of this study are exploratory.

2.2 Study hypotheses

Primary objective: MRI measurements of tumour hypoxia levels directly correlate to measurements of [¹⁸F]MISO PET uptake.

Secondary objective 1: MRI measurements of hypoxia in the tumour volume acquired in the test-retest scans have excellent repeatability.

Secondary objective 2: Dose-painting radiotherapy plans that target areas of hypoxic tumour with high doses of radiation will result in improved modelled local tumour control probability and minimal alteration to normal tissue dose tolerances compared to standard radiotherapy plans.

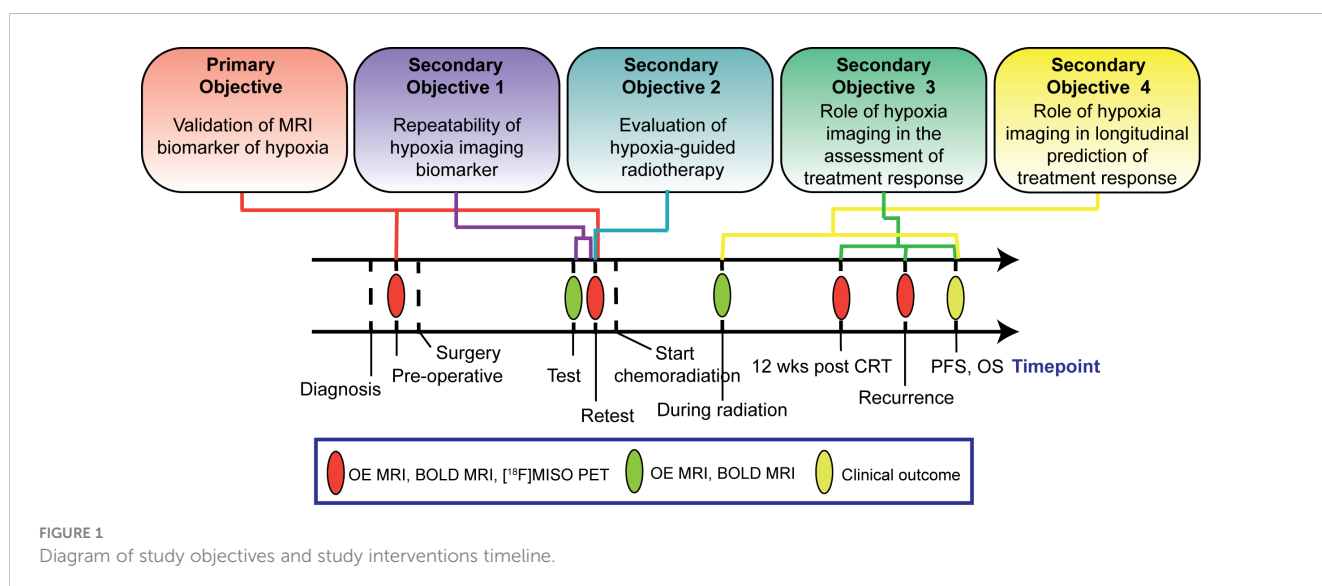
Secondary objective 3: MRI measurements of tumour hypoxia at 12 weeks post chemoradiation treatment completion spatially overlap with sites of local recurrence and negatively correlate with patient overall survival time.

Secondary objective 4: Increases in measurements of tumour hypoxia observed during chemoradiation treatment negatively correlate with patient overall survival time.

2.3 Study outcome measures

2.3.1 Primary objective

Spatial correlation between hypoxic tumour volume (HTV) determined with MRI and [¹⁸F]MISO will be evaluated via measurements of Dice similarity coefficient. Dice similarity coefficients > 0.75 will be considered a good spatial correlation. Quantitative correlation of voxel-wise and HTV-average levels of hypoxia will be evaluated via measurement of the Pearson's correlation coefficient. Correlation coefficients > 0.7 will be considered a strong correlation (27).



2.3.2 Secondary objective 1

Repeatability of voxel-wise and HTV-average levels of hypoxia in the tumour, calculated as explained below for each hypoxia imaging biomarker, will be assessed via measurements of intraclass correlation coefficient (ICC). Repeatability is considered excellent, good, moderate or poor for ICC values > 0.9 , $0.75-0.9$, $0.5-0.75$ and < 0.5 , respectively. Additionally, similarity between the HTV defined with the MRI biomarker at the two timepoints will be assessed via calculation of Dice similarity coefficient. Dice similarity coefficients > 0.9 will be considered a strong correlation.

2.3.3 Secondary objective 2

The predicted patient benefits of the hypoxia-guided dose-painting radiotherapy plan will be compared with the actual patient outcomes following conventional treatment, by using metrics including modelled tumour control probability (TCP) and toxicity measurement to organs at risks and healthy brain (including equivalent uniform dose). Voxel-wise dose-painting prescriptions within the conventional radiotherapy targets will be escalated from 60 Gy based on the level of hypoxia determined by the selected MRI imaging biomarker according to the method previously described by Toma-Dasu et al. (28). Targets delineation and constraints to organs at risk as per ESTRO-EANO guidelines (29) will be set equally for the optimisation of the conventional and dose-painting plans. Success for this objective will be achieved if the dose-painting plans result in improved TCP by more than 15% over conventional treatment, while dose metrics to organs at risk remain similar.

2.3.4 Secondary objective 3

Spatial correlation between HTV after completion of chemoradiation treatment and volume of recurrent tumour at relapse evaluated with standard anatomical imaging will be evaluated via measurements of Dice similarity coefficient. Dice similarity coefficients > 0.9 will be considered a strong spatial correlation. Correlation between the percentage of HTV after completion of chemoradiation treatment and clinical outcome will be evaluated by means of hazard ratio obtained from Cox regression. A hazard ratio > 1 ($p < 0.05$) will indicate that the HTV at suspected recurrence is associated with worse patient overall survival.

2.3.5 Secondary objective 4

Correlation between the percentage change of HTV during treatment and patient clinical outcome will be evaluated by means of hazard ratio obtained from Cox regression. A hazard ratio > 1 ($p < 0.05$) will indicate that the increase in HTV during treatment is associated with worse patient overall survival. Given the known prognostic role of sex and age on GBM overall survival (30–32), sub-analyses assessing whether HTV increase during treatment has a sex/age-specific impact on overall survival will be performed.

2.4 Study design

This study is a non-randomised, uncontrolled, non-interventional, prospective imaging study.

This study will enrol patients with radiological diagnosis of grade IV glioma and for whom a diagnosis of glioblastoma, IDH wild type is confirmed on neuropathological exam, according to the WHO 2021 glioma classification criteria (33). Patients fulfilling the inclusion criteria will receive standard of care treatment according to the Stupp protocol (34), with the addition of OE and BOLD MRI and [^{18}F]MISO PET scans to routine diagnostic protocols (Figure 2). MRI scans employing OE and BOLD sequences, as well as [^{18}F]MISO PET/CT scans, will be acquired for patients pre-operatively at diagnosis, prior to commencement of chemoradiation treatment (3–4 weeks post-operative) and 12 weeks following completion of radiotherapy. Supplementary OE and BOLD MRI scans will also be performed in a test/retest setting prior to commencement of radiotherapy as well as during radiotherapy if the patients are amenable. If there is suspected recurrence on long term MRI surveillance, patients will be invited for repeat OE/BOLD MRI and [^{18}F]MISO PET/CT scans. [^{18}F]MISO PET imaging will be used to establish ground truth presence of hypoxia in the tumour. Existing correlations between MRI-derived levels of hypoxia and hypoxia levels assessed via [^{18}F]MISO PET uptake will be evaluated (35–39). This study will require recruitment of a sample of 20 patients, as in previous clinical trials (NCT03716986, NCT02466828 and NCT00906893).

2.5 Study setting

In total, two sites will be utilised on the Northern Sydney Local Health District, Sydney, NSW, Australia: Royal North Shore Hospital (RNSH) and North Shore Radiology (NSR). Patients presenting with radiological symptoms of high-grade glioma at either of these sites will be presented with the opportunity to enrol in this study. This study is expected to recruit 20 patients. Following initial recruitment, NSR will be the site at which all the MRI scans will be performed, while RNSH will be the site at which the PET scans will be performed. Consent procedures may be performed at either site.

2.6 Selection of subjects

2.6.1 Inclusion criteria

Male and female patients aged 18 years or older with suspected high-grade glioma at initial radiological examination and confirmed neuropathological diagnosis of glioblastoma, IDH wild type according to the WHO 2021 glioma classification criteria (33) will be recruited. Qualifying patients must have an Eastern Cooperative Oncology Group (ECOG) performance status score of 0–2, be available for scanning on two separate days and provide written informed consent for participation in this trial once eligibility is met.

2.6.2 Exclusion criteria

- Women lactating, pregnant or of childbearing potential who are not willing to avoid pregnancy during the study

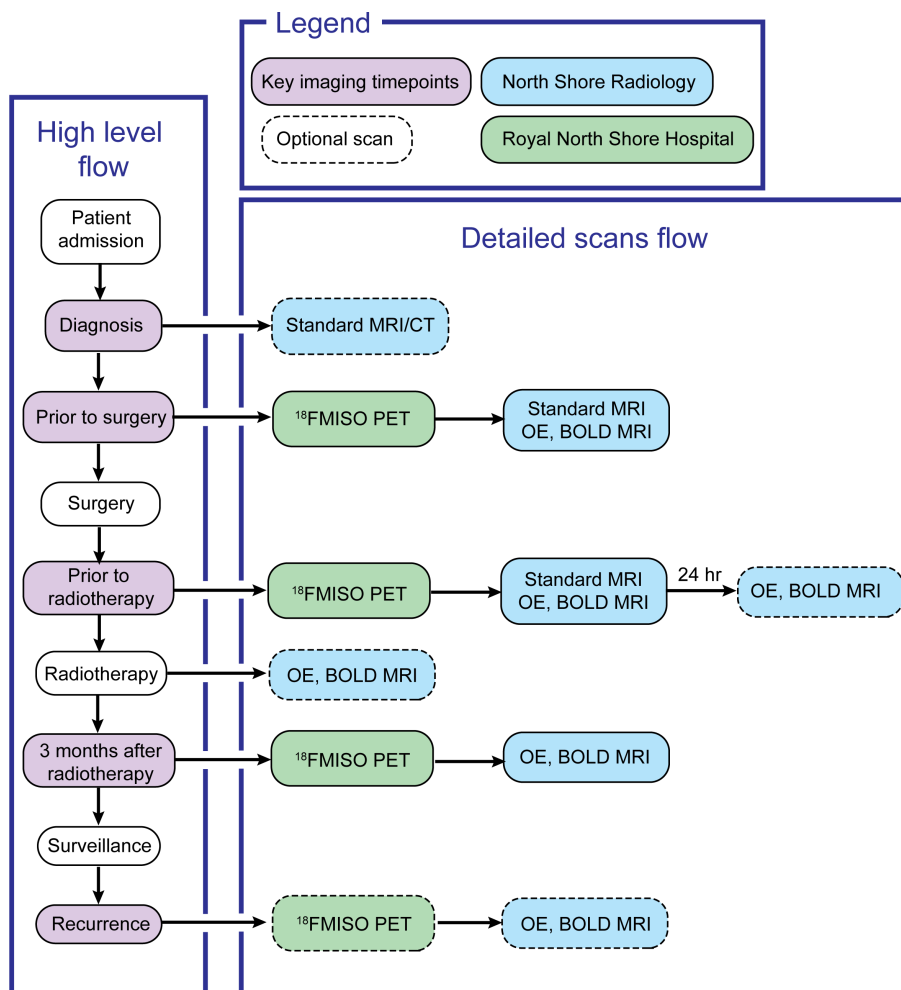


FIGURE 2
Diagram of study interventions flowchart.

- Patients with a history of severe renal disease(s) (eGFR<20) who cannot tolerate gadolinium chelate contrast agents
- Neuropathological diagnosis not consistent with glioblastoma IDH wild type
- Geographically remote patients unable to agree to imaging schedule
- Patients who have received anti-VEGF monoclonal antibody therapy within 3 months prior to recruitment
- Patients with a history of psychological illness or condition such as to interfere with the patient’s ability to understand the requirements of the study
- Patients with significant cardiac or pulmonary disease including cardiac arrhythmias or Chronic Obstructive Pulmonary Disease (COPD) that are unable to tolerate high flow O₂ for oxygen contrast.
- Patients taking carbonic anhydrase inhibitors (Acetazolamide)
- History of glaucoma
- Any contraindication to MRI imaging.

2.7 Interventional methods

2.7.1 MRI protocol

At each of the imaging timepoint determined in the study design patients will undergo the following MRI scans (Figure 3):

- OE MRI: including T₁ mapping sequence prior to oxygen challenge, T₁-weighted dynamic sequence (40) during oxygen challenge, T₁ mapping sequence during oxygen challenge;
- BOLD MRI: T₂ mapping sequence, T₂* mapping sequence, T₂* dynamic sequence during oxygen switch off, DSC sequence with single bolus of gadolinium-based contrast agent.

MRI scans will be acquired on Siemens 3T systems (Vida) with a 64-channels head coil.

Details of the MRI sequences acquisition parameters are collected in Table 1. T₁-weighted dynamic imaging will be

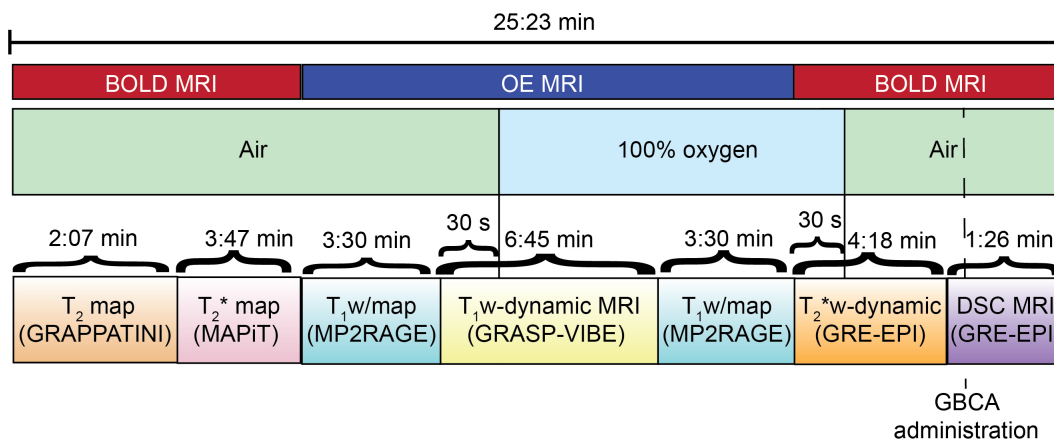


FIGURE 3 Schematic of oxygen delivery protocol and MRI sequences acquisition.

performed with a golden-angle radial sparse parallel-volumetric interpolated breath-hold (GRASP-VIBE) that permits reconstruction of image volumes at retrospectively determined temporal resolution (40). The DSC MRI sequence will be acquired to characterize tissue perfusion, which will be important in the analysis of MRI/PET images to identify regions of the tumour where hypoxia is not induced by poor tissue perfusion (41).

During OE MRI acquisition patients will sequentially breathe medical air and 100% O₂ (up to 15 l/min) through nasal prongs or oxygen mask. During DSC sequence acquisition, patients will be injected intravenously with a dose of 0.1 mmol/kg gadolinium-based contrast agent (GBCA) at a rate of 3-5 ml/s.

2.7.2 MRI analysis

Quantitative T₁, T₂ and T₂* maps will be derived from in-line processing of the T₁-mapping, T₂-mapping and T₂*-mapping sequences, respectively, available on the scanner as part of the Siemens license agreement. Examples of quantitative images obtained from a healthy volunteer are shown in Figure 4. T₁ maps for each timepoint of the T₁-weighted dynamic acquisition will be

calculated from static T₁ maps by assuming that signal changes are due to T₁ effects only, which is reasonable for sequences with very short echo times. These T₁ maps calculations will be performed via an in-house software and a commercially available brain tumour imaging software, IB DCE (Imaging Biometrics LLC, Elm Grove, WI, USA). Cerebral blood flow (CBF) and cerebral blood volume (CBV) maps will be derived from kinetics modelling of the DSC data performed using the industry-leading brain tumour imaging software, IB Neuro (Imaging Biometrics LLC, Elm Grove, WI, USA).

A region of interest (ROI) will be delineated with a semi-automated tool and checked by an experienced neuroradiologist on the T₂-weighted image as the hyperintense regions around the tumour. The ROI will be propagated to the T₁, T₂, T₂* and CBF maps. Voxel-wise and median values of R₁, R₂, R₂* and CBF within the ROI will be calculated from the quantitative T₁, T₂, T₂* and CBF maps, respectively. The reproducibility, repeatability and accuracy of the quantitative-MRI protocol will also be assessed using guidelines and a phantom developed by the National Institute of Standards and Technology and the International Society of Magnetic Resonance in Medicine (42).

TABLE 1 MRI scan protocol acquisition parameters on a Siemens 3T scanner.

Parameter	T ₁ mapping + T13D (MP2RAGE)	T ₁ w-dynamic (GRASP-VIBE)	T ₂ mapping (GRAPPATINI)	T ₂ * mapping (MAPiT)	T ₂ *w- dynamic (GRE-EPI)	DSC (GRE-EPI)
Acquisition time	3:30 min	6:45 min	2:07 min	3:47 min	4:18 min	1:26 min
Resolution (mm ³)	1×1×1	1×1×1	0.7×0.7×4.0	1.7×1.7×4.0	1.7×1.7×4.0	1.7×1.7×4.0
Matrix size	240×256×192	256×256×104	320×240×30	128×128×30	128×128×20	128×128×20
TR (ms)	5000	4.51	5000	880	1230	1230
TE (ms)	2.9	1.65	16 TEs, TE1 = 10 ms, TE step=10 ms	12 TEs, TE1 = 6 ms, TE step=5 ms	30	30
Flip angle	0°	2°	180°	30°	90°	90°
Number of averages	1	1	1	1	1	1

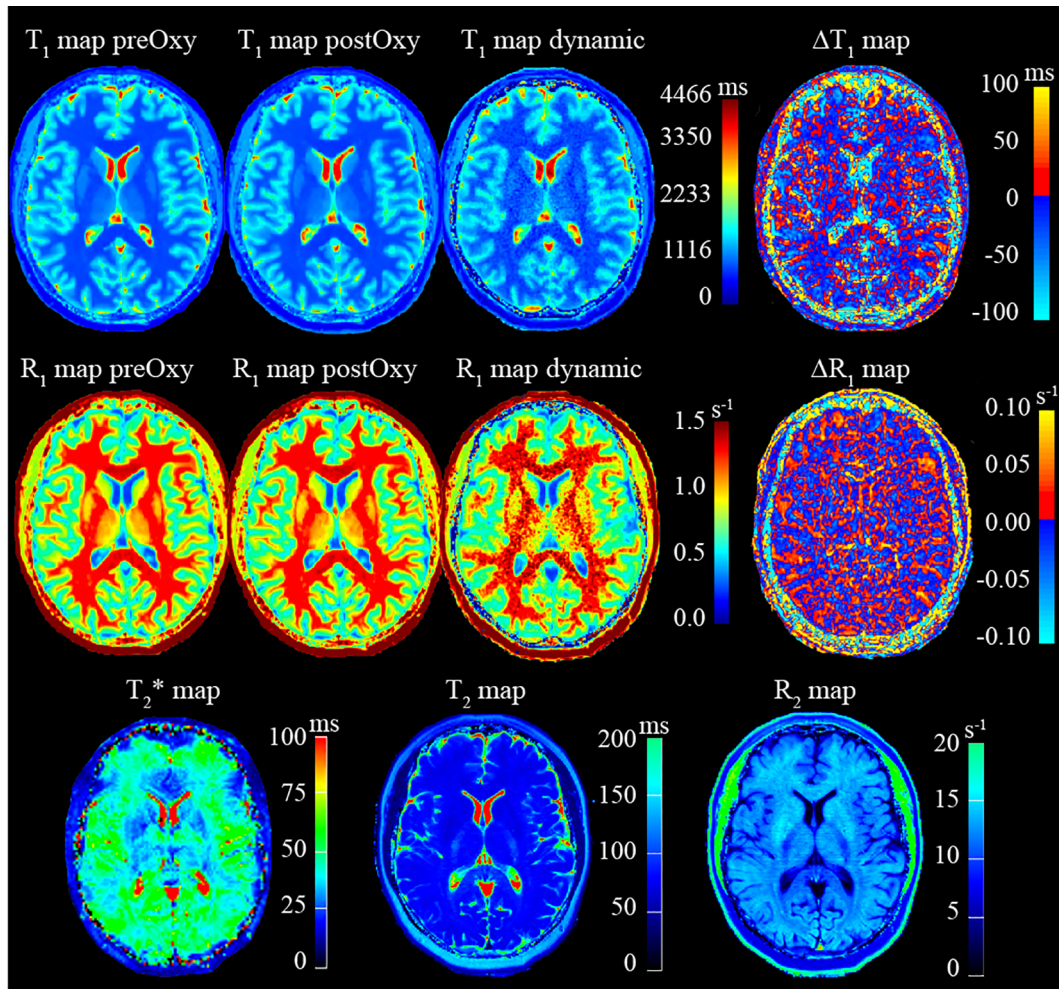


FIGURE 4 Example of quantitative images obtained from MRI protocol acquisition on a healthy volunteer.

On one hand, HTV will be defined via OE MRI as the proportion of voxels within the ROI being refractory in R_1 for O_2 challenge [i.e. $\Delta R_1 \leq 0$, where $\Delta R_1 = R_1(O_2) - R_1(\text{air})$] and well-perfused (i.e. $CBF > 0$), as previously determined by experts in the field (36, 41, 43, 44). ΔR_1 will be calculated in two ways. First, it will be calculated from the R_1 maps obtained from the T_1 -mapping sequences acquired before [$R_1(\text{air})$] and during O_2 breathing [$R_1(O_2)$]. Second, it will be calculated from T_1 maps derived from the T_1 -weighted dynamic acquisition, such that $R_1(\text{air})$ is derived from the average of the first two R_1 maps acquired at baseline while breathing air and $R_1(O_2)$ is derived from the last four R_1 map acquired during oxygen breathing. ΔR_1 values obtained with the two approaches will be compared. The approach which will provide the most reliable ΔR_1 values in the test-retest scan across the entire patient cohort will then be selected to calculate the HTV. Voxel-wise ΔR_1 values in the HTV will be converted into values of partial pressure of oxygen (pO_2) using a similar approach to the one used by Chakhoyan et al. (35), which exploits known values of pO_2 in normal appearing white and gray matter and uses these values to calibrate the pO_2 values in the tumour. This approach will provide a way to quantitatively measure voxel-wise levels of hypoxia.

On the other hand, HTV will be defined via BOLD MRI by using a previously established method to estimate relative oxygen extraction fraction (rOEF) in human gliomas from T_2 , T_2^* and CBV maps (37). Briefly, the transverse relaxation due to local magnetic field inhomogeneities in a blood vessel network, R_2' , will be calculated within the ROI from T_2 and T_2^* maps according to Equation 1:

$$R_2' = R_2^* - R_2 = \left(\frac{1}{T_2^*} - \frac{1}{T_2} \right) \tag{1}$$

Then, the Yablonskiy and Haacke model will be applied to derive the oxygen extraction fraction (OEF) according to Equation 2:

$$OEF = \frac{R_2'}{\zeta \cdot \gamma \cdot \frac{4}{3} \cdot \pi \cdot \Delta\chi \cdot B_0} \tag{2}$$

where ζ is the venous fraction of the blood network and approximately equals the venous blood volume ($\sim 0.75 \cdot CBV$), B_0 is the magnetic field strength, γ is the gyromagnetic ratio of value $2.675 \cdot 10^8 \text{ s}^{-1} \text{ T}^{-1}$, $\Delta\chi$ is the susceptibility difference between deoxygenated and oxygenated blood $\Delta\chi = \Delta\chi_0 \cdot Hct = 0.924 \cdot 10^{-7}$, which is

calculated from the susceptibility difference between fully deoxygenated and fully oxygenated hemoglobin $\Delta\chi_0 = 0.264 \cdot 10^{-6}$ and the small-vessel hematocrit (Hct = 0.35). As the absolute quantification of venous CBV in patients is not feasible, the venous blood vessel fraction ζ is approximated by CBV and the remaining factors are grouped into a constant $c = \gamma \cdot \frac{4}{3} \cdot \pi \cdot \Delta\chi \cdot B_0 = 317 \text{ s}^{-1}$. Using these simplifications, rOEF can be calculated according to Equation 3:

$$rOEF = \frac{R_2'}{CBV \cdot c} = \left(\frac{1}{T_2^*} - \frac{1}{T_2} \right) \cdot \frac{1}{CBV \cdot c} \quad (3)$$

To derive the HTV, a hypoxia rOEF threshold (rOEF_{hypoxia}) will be defined from the mean, rOEF_{mean}, and the standard deviation, rOEF_{SD}, of the tissue within the ROI, such that rOEF_{hypoxia} = rOEF_{mean} + rOEF_{SD}. Finally, the HTV will be defined by all voxels within the ROI for which rOEF > rOEF_{hypoxia}. Hypoxia levels in voxels belonging to the HTV will be measured by rOEF values.

To facilitate the assessment of spatial and quantitative voxel-wise correlations in HTV and in levels of tumour hypoxia defined by the different imaging biomarkers, all MRI images will be resampled into the spatial resolution of the MRI image with the highest resolution by linear interpolation of voxel-wise intensity values.

2.7.3 PET imaging protocol

At multiple timepoints determined in the study design (i.e. pre-op, once prior to commencement of chemoradiation and at suspected recurrence) the patients will also undergo a [¹⁸F]MISO PET/CT scan. Patients will be requested to come to the department 2 hours prior to the scan session. The amount of [¹⁸F]MISO given will be 370 MBq administered intravenously approximately 90 min prior to imaging. The PET data will be reconstructed to provide trans-axial images using standard protocols and the lesion uptake will be evaluated.

2.7.4 PET imaging analysis

PET data will be reconstructed with CT data acquired simultaneously. To quantify the radioactivity concentrations in the PET images as standardised uptake values (SUV), raw PET images will be decay corrected to the point of tracer injection using a fluorine-18 half-life of 109.77 min. PET images will be co-registered to the MRI images acquired at the same timepoint of the study via rigid co-registration of the simultaneously acquired CT image to the T₂ map. This way the ROI delineated on the T₂ image can be applied to the PET SUV image and be used for quantification of lesion [¹⁸F]MISO uptake. The primary measures to quantify lesion [¹⁸F]MISO uptake will be maximum standardised uptake value (SUV_{max}) and tumour-to-background ratios (TBR). TBR images will be derived by normalisation of the SUV image by the mean SUV value calculated in a region of interest delineated in the contralateral healthy brain. The HTV will be defined by all voxels within the tumour ROI with a TBR ≥ 1.2 - threshold value shown to optimally distinguish hypoxic tumour from normoxic brain tissue at 90 min post tracer injection in a previous GBM study (45) – and DSC MRI-derived CBF > 0 – indicating well-perfused tissue. Hypoxia levels in voxels belonging to the HTV will be

measured by values of pO₂ derived from TBR values using the above mentioned approach used by Chakhoyan et al. (35).

Finally, to facilitate the assessment of spatial and quantitative voxel-wise correlations in HTV and in levels of tumour hypoxia defined by the different imaging biomarkers, [¹⁸F]MISO TBR images will be resampled into the spatial resolution of the MRI image with the highest resolution by linear interpolation of voxel-wise intensity values.

2.7.5 Preparation and administration of [¹⁸F]MISO

Fluorine-18 will be sourced from a local PET radiopharmacy (Cyclotek NSW, Lucas Heights, Sydney). [¹⁸F]MISO will be synthesized on-site at RNSH using the ABX Products PE-SC-12, PE-TBA-001.750, PE-VVIAL-016 and the SCINTOMICS GRP[®] Synthesizer. Cartridge purification will be carried out as part of the automated synthesis procedure programmed by Scintomics and ABX. ITLC and HPLC quality controls will be carried out post-synthesis and prior to release for patient administration. The pass mark for both HPLC and ITLC is >95%. The average QC results achieved for radiotracers produced at the RNSH facility are >98%. Following purification and characterisation procedures, a diagnostic dose of approximately 370 MBq ± 10% of [¹⁸F]MISO will be administered to patients via intravenous injection.

2.8 Data collection, storage, confidentiality and retention

There will be general information recorded about the patient including patient size (height and weight).

The following radiographic and radiotherapy-specific data will be collected for each patient:

- MRI images as DICOM series and raw k-space data in the proprietary vendor format
- [¹⁸F]MISO PET and CT data and reconstructed images as DICOM series
- Radiotherapy planning contours
- Radiotherapy treatment plans
- Clinical data including progression-free survival and overall survival

Patients enrolled in the study will receive a trial ID. The data saved for the trial will be under this de-identified trial ID. A separate key of the subject study number and their medical record number will be securely stored by the clinical trials staff to allow re-identification if necessary. This master list for re-identification will remain at RNSH. Only the clinical trials staff will have the ability to re-identify subjects. The data will be stored for 15 years as per Good Clinical Practice (GCP) guidelines. Imaging and clinical outcome data will be transferred from RNSH to the University of Sydney using a password protected cloud-based file share solutions from Citrix ShareFile, in accordance with the study site's ethics and security allowances and protocols. The de-identified data will be stored for 15 years at the University of Sydney on a secure, password protected backed up storage drive (Research Data Storage). Only non-identifiable data may be made available for other

scientific research, e.g., nonidentifiable data placed on a well-controlled university site, upon request. The data sharing platform is a secure on-line storage solution (“CloudStor”) provided through the University of Sydney. The data will be stored as a password-protected, encrypted file. In order to download or decompress the data, participating researchers will agree to the terms of use for the data, including that the data is not to be published or otherwise redistributed without the express consent of the original investigators.

2.9 Adverse event reporting and management

All adverse events related to the administration of oxygen for OE MRI and [¹⁸F]MISO for the PET imaging procedures will be reported to the Trial Management Committee and reviewed as to requirement for reporting to the institution ethics review board. Determination of the severity of adverse events will be consistent with Common Terminology Criteria for Adverse Events (version 5). The relationship between an adverse event and the investigational product will be determined by the Investigator. An event should be considered related to treatment if, in the clinical principal investigator’s medical judgment, there is a reasonable possibility that the event may have been caused by the study drug. The investigator will be responsible for ensuring that any adverse events observed by the investigator or reported by the subject are recorded in the subject’s medical record and reported.

Scans will be stopped if suspected adverse drug reactions, changes in vital signs, electrocardiogram, or clinical laboratory results are observed and these changes pose a significant health risk. Clinically or medically significant suspected adverse drug reactions, and serious adverse events considered to be related to study procedures will be followed until resolved or considered stable. Subjects withdrawn from the study will be treated as deemed appropriate by the treating physician. Safety follow-up procedures will be performed and the appropriate Clinical Research Facilities will be completed.

2.10 Statistical analysis

The sample size required for this study was calculated from a power analysis performed with the software GPower v.3.1. based on the hypothesis linked to the primary objective of the study. The hypothesis is that OE and BOLD MRI measurements of hypoxia within the tumour lesion will positively correlate (Pearson correlation coefficient > 0.7) to [¹⁸F]MISO values of uptake. The statistical test used in the power analysis was a correlation test using a point biserial model. Based on a Pearson correlation coefficient of 0.7, which was previously reported for the correlation of MRI measurements of hypoxia and the gold-standard immunohistochemical marker of hypoxia pimonidazole (27), the minimum sample size required to answer the hypothesis with 98% power and 5% two-tailed alpha, is 19. As such, up to 20 patients will be recruited for this study. A sample size of N=20 patients, which is large compared to the usual sample size used to estimate repeatability of ROI-averaged quantitative imaging measures (46), will allow us to test the hypothesis linked to secondary objective 1 - involving assessing the

repeatability of OE/BOLD MRI measurements of hypoxia with the test-retest scan - with a specificity of at least 85% with 95% certainty (47); and the hypothesis linked to secondary objective 2 - involving the assessment of whether dose-painting radiotherapy plans result in improved TCP by more than 15% over conventional treatment - with 99% power and 5% one-tailed alpha (calculated with GPower v.3.1.).

3 Discussion

This diagnostic/prognostic imaging study will enable validation of the role of non-invasive MRI biomarkers of hypoxia that could be used to improve diagnosis, radiation treatment, prognosis and treatment response assessment of GBM patients. This study is ambitious in that it aims to characterise the evolution of tumour hypoxia levels during the whole course of patient management pipeline, with a plan to acquire MRI and PET/CT scans pre-operatively at diagnosis, prior to commencement of chemoradiation treatment, 12 weeks following completion of radiotherapy and at suspected diagnosis of recurrence, and supplementary MRI scans in a test-retest setting prior to commencement of radiotherapy and during radiotherapy. The supplementary MRI scans, which are required to test hypothesis for secondary objectives 1 and 4, will be considered optional based on patients’ status and compliance. Similarly, patients will be invited for repeat OE/BOLD MRI and [¹⁸F]MISO PET/CT scans only in case of suspected recurrence on long term MRI surveillance, meaning that there might only be a subset of patients whose data will be used to test hypothesis of secondary objective 3. Nonetheless, this study will generate a large amount of longitudinal multimodal MRI and PET imaging data that will be extremely valuable to unveil important dynamic changes in tumour physiology that currently limit treatment efficacy, thereby providing a means to develop more effective, personalised treatment strategies.

It is worth mentioning that one potential limitation in our study design is the challenge of including a selection criterium to ensure that the cohort of patients enrolled in the study exhibits different levels of hypoxia. This is important to ensure a more robust evaluation of the correlation between the OE/BOLD MRI biomarkers of hypoxia and [¹⁸F]MISO uptake levels. However, achieving such patients selection prior to enrolment in the study is neither trivial nor feasible in our study, because it would require quantification of hypoxia tumour levels via [¹⁸F]MISO PET scan, which is not performed as a routine standard-of-care diagnostic scan at our clinical centre. We mitigated the risk of this potential limitation by considering the typical incidence of hypoxia levels in GBM tumours. We looked at the results of a previously published clinical study quantifying regional levels of hypoxia in newly diagnosed GBM patients with [¹⁸F]MISO PET (12). This study enrolled 22 patients who had varying hypoxic tumour volumes (range: 0.1-129.3 cm³, median: 12.85 cm³) and heterogeneous levels of hypoxia (range T/B_{max}: 1.2-4.2, median: 4.05). As we aim to recruit a similar number of patients with the same pathology, we assume to recruit a cohort of patients with similar hypoxia tumour volume/levels characteristics. It will certainly be important to report these metrics in our study results.

Moreover, we acknowledge that in our study we reserve the option of using either nasal prongs or a non-rebreather face mask for the

delivery of oxygen gas in the OE MRI protocol. The choice for the oxygen delivery method will be linked to the feasibility of fitting the non-rebreather mask into the 64-channel MRI head coil that will be used in the study. The use of nasal prongs, which may be necessary for patients for whom a face mask would not fit comfortably into the head coil, could potentially limit the fractions of inspired oxygen (FiO_2) to approximately 40%, hence resulting into a low OE MRI signal-to-noise ratio. We have mitigated this risk by testing our OE MRI protocol on a healthy volunteer who received oxygen delivery via nasal prongs. The ΔR_1 measured in the nasal concha was $0.04 \pm 0.04 \text{ s}^{-1}$, which is comparable to the ΔR_1 of $0.05 \pm 0.02 \text{ s}^{-1}$ observed in the same region of interest in healthy subjects in a similar OE MRI study using a non-rebreather oxygen mask (48). This result suggests that a similar hyper-oxygenation effect in the tissue could be achieved either by use of nasal prongs or non-rebreather face mask. Notably, validating that OE MRI can identify regions of tumour hypoxia by using nasal prongs for oxygen delivery would have higher impact in the widespread clinical translation of this method, as nasal prongs are safe, not limited by coil design or head shape, routinely used and widely available to all clinical centres.

Ethics statement

All patients enrolled in the study are to provide written informed consent in accordance with institutional guidelines. Ethics approval for this study was obtained from the Northern Sydney Local Health District Human Research Ethics Committee on 15 April 2022: registration number 2021/ETH11794. This covers all participating clinical sites, including the Royal North Shore Hospital (RNSH) and North Shore Radiology (NSR).

Author contributions

CB: Conceptualization, Data curation, Formal analysis, Investigation, Methodology, Project administration, Resources, Software, Supervision, Validation, Writing – original draft, Writing – review & editing. DW: Conceptualization, Funding acquisition, Investigation, Methodology, Resources, Software, Writing – review & editing. PK: Conceptualization, Writing – review & editing. JB:

Conceptualization, Writing – review & editing. KO'B: Conceptualization, Resources, Software, Writing – review & editing. SS: Writing – review & editing, Project administration. JP: Funding acquisition, Writing – review & editing, Conceptualization. MM: Methodology, Writing – review & editing, Resources. JY: Funding acquisition, Writing – review & editing, Project administration. DB: Conceptualization, Methodology, Writing – review & editing. MB: Conceptualization, Funding acquisition, Writing – review & editing. JD: Conceptualization, Funding acquisition, Investigation, Methodology, Project administration, Resources, Writing – review & editing.

Funding

The author(s) declare financial support was received for the research, authorship, and/or publication of this article. This trial is funded by The Brain Cancer Group, St Leonards, Australia. DW is supported by a Cancer Institute NSW Early Career Fellowship 2019/ECF1015. CB received salary support for this work from the Australian National Health and Medical Research Council Program Grant APP1132471.

Conflict of interest

Authors KO'B and MM was employed by the company Siemens Healthcare Pty Ltd.

The remaining authors declare that the research was conducted in the absence of any commercial or financial relationships that could be construed as a potential conflict of interest.

Publisher's note

All claims expressed in this article are solely those of the authors and do not necessarily represent those of their affiliated organizations, or those of the publisher, the editors and the reviewers. Any product that may be evaluated in this article, or claim that may be made by its manufacturer, is not guaranteed or endorsed by the publisher.

References

- Jayamanne D, Wheeler H, Cook R, Teo C, Brazier D, Schembri G, et al. Survival improvements with adjuvant therapy in patients with glioblastoma. *ANZ J Surg* (2018) 88(3):196–201. doi: 10.1111/ans.14153
- Jungk C, Warta R, Mock A, Friauf S, Hug B, Capper D, et al. Location-dependent patient outcome and recurrence patterns in IDH1-wildtype glioblastoma. *Cancers (Basel)*. (2019) 11(1):1–17. doi: 10.3390/cancers11010122
- Jiang H, Yu K, Li M, Cui Y, Ren X, Yang C, et al. Classification of progression patterns in glioblastoma: analysis of predictive factors and clinical implications. *Front Oncol* (2020) 10(November):1–11. doi: 10.3389/fonc.2020.590648
- Valdebenito S, D'Amico D, Eugenin E. Novel approaches for glioblastoma treatment: Focus on tumor heterogeneity, treatment resistance, and computational tools. *Cancer Rep* (2019) 2(6):1–13. doi: 10.1002/cnr2.1220
- Chédeville AL, Madureira PA. The role of hypoxia in glioblastoma radiotherapy resistance. *Cancers (Basel)* (2021) 13(3):542. doi: 10.3390/cancers13030542
- Gerstner ER, Zhang Z, Fink JR, Muzi M, Hanna L, Greco E, et al. ACRIN 6684: assessment of tumor hypoxia in newly diagnosed glioblastoma using 18F-FMISO PET and MRI. *Clin Cancer Res* (2016) 22(20):5079–86. doi: 10.1158/1078-0432.CCR-15-2529
- Cher LM, Murone C, Lawrentschuk N, Ramdave S, Papenfuss A, Hannah A, et al. Correlation of hypoxic cell fraction and angiogenesis with glucose metabolic rate in gliomas using 18F-fluoromisonidazole, 18F-FDG PET, and immunohistochemical studies. *J Nucl Med* (2006) 47(3):410–8.
- Muzi M, Wolsztynski E, Fink JR, O'sullivan JN, O'sullivan F, Krohn KA, et al. Assessment of the prognostic value of radiomic features in 18F-fmiso pet imaging of hypoxia in postsurgery brain cancer patients: Secondary analysis of imaging data from

a single-center study and the multicenter acrin 6684 trial. *Tomography* (2020) 6(1):14–22. doi: 10.18383/j.tom.2019.00023

9. Ratai E-M, Zhang Z, Fink J, Muzi M, Hanna L, Greco E, et al. ACRIN 6684: Multicenter, phase II assessment of tumor hypoxia in newly diagnosed glioblastoma using magnetic resonance spectroscopy. *PLoS One* (2018) 13(6):e0198548. doi: 10.1371/journal.pone.0198548

10. Carlson DJ, Yenice KM, Orton CG. Tumor hypoxia is an important mechanism of radioresistance in hypofractionated radiotherapy and must be considered in the treatment planning process. *Med Phys* (2011) 38(12):6347–50. doi: 10.1118/1.3639137

11. Leimgruber A, Hickson K, Lee ST, Gan HK, Cher LM, Sachinidis JJ, et al. Spatial and quantitative mapping of glycolysis and hypoxia in glioblastoma as a predictor of radiotherapy response and sites of relapse. *Eur J Nucl Med Mol Imaging* (2020) 47(6):1476–85. doi: 10.1007/s00259-020-04706-0

12. Spence AM, Muzi M, Swanson KR, O'Sullivan F, Rockhill JK, Rajendran JG, et al. Regional hypoxia in glioblastoma multiforme quantified with [18F] fluoromisonidazole positron emission tomography before radiotherapy: Correlation with time to progression and survival. *Clin Cancer Res* (2008) 14(9):2623–30. doi: 10.1158/1078-0432.CCR-07-4995

13. Hirata K, Yamaguchi S, Shiga T, Kuge Y, Tamaki N. The roles of hypoxia imaging using 18F-fluoromisonidazole positron emission tomography in glioma treatment. *J Clin Med* (2019) 8(8):1088. doi: 10.3390/jcm8081088

14. Carrete LR, Young JS, Cha S. Advanced imaging techniques for newly diagnosed and recurrent gliomas. *Front Neurosci* (2022) 16(February):2–18. doi: 10.3389/fnins.2022.787755

15. Gérard M, Corroyer-Dulmont A, Lesueur P, Collet S, Chérel M, Bourgeois M, et al. Hypoxia imaging and adaptive radiotherapy: A state-of-the-art approach in the management of glioma. *Front Med* (2019) 6:117/full(June). doi: 10.3389/fmed.2019.00117/full

16. Yamaguchi S, Hirata K, Toyonaga T, Kobayashi K, Ishi Y, Motegi H, et al. Change in 18 F-Fluoromisonidazole PET Is an early predictor of the prognosis in the patients with recurrent high-grade glioma receiving bevacizumab treatment. *PLoS One* (2016) 11(12):1–15. doi: 10.1371/journal.pone.0167917

17. Mendichovszky I, Jackson A. Imaging hypoxia in gliomas. *Br J Radiol* (2011) 84(2):145–58. doi: 10.1259/bjr/82292521

18. Albert NL, Weller M, Suchorska B, Galdiks N, Soffietti R, Kim MM, et al. Response Assessment in Neuro-Oncology working group and European Association for Neuro-Oncology recommendations for the clinical use of PET imaging in gliomas. *Neuro Oncol* (2016) 18(9):1199–208. doi: 10.1093/neuonc/now058

19. Wen PY, Weller M, Lee EQ, Alexander BM, Barnholtz-Sloan JS, Barthel FP, et al. Glioblastoma in adults: A Society for Neuro-Oncology (SNO) and European Society of Neuro-Oncology (EANO) consensus review on current management and future directions. *Neuro Oncol* (2020) 22(8):1073–113. doi: 10.1093/neuonc/noaa106

20. Pope WB, Brandal G. Conventional and advanced magnetic resonance imaging in patients with high-grade glioma. *Q J Nucl Med Mol Imaging*. (2018) 62(3):239–53. doi: 10.23736/S1824-4785.18.03086-8

21. Keall PJ, Brighi C, Glide-Hurst C, Liney G, Liu PZY, Lydiard S, et al. Integrated MRI-guided radiotherapy — opportunities and challenges. *Nat Rev Clin Oncol* (2022) 19(7):458–70. doi: 10.1038/s41571-022-00631-3

22. Zhou H, Chiguru S, Hallac RR, Yang D, Hao G, Peschke P, et al. Examining correlations of oxygen sensitive MRI (BOLD/TOLD) with [18F]FMISO PET in rat prostate tumors. *Am J Nucl Med Mol Imaging* (2019) 9(2):156–67.

23. White DA, Zhang Z, Li L, Gerberich J, Stojadinovic S, Peschke P, et al. Developing oxygen-enhanced magnetic resonance imaging as a prognostic biomarker of radiation response. *Cancer Lett* (2016) 380(1):69–77. doi: 10.1016/j.canlet.2016.06.003

24. Arai TJ, Yang DM, Campbell JW, Chiu T, Cheng X, Stojadinovic S, et al. Oxygen-sensitive MRI: A predictive imaging biomarker for tumor radiation response? *Int J Radiat Oncol Biol Phys* (2021) 110(5):1519–29. doi: 10.1016/j.ijrobp.2021.03.039

25. Beeman SC, Shui YB, Perez-Torres CJ, Engelbach JA, Ackerman JJH, Garbow JR. O2-sensitive MRI distinguishes brain tumor versus radiation necrosis in murine models. *Magn Reson Med* (2016) 75(6):2442–7. doi: 10.1002/mrm.25821

26. Lickliter JD, Ruben J, Kichenadasse G, Jennens R, Gzell C, Mason RP, et al. Dodecafluoropentane emulsion as a radiosensitizer in glioblastoma multiforme. *Cancer Res Commun* (2023) 3(8):1607–14. doi: 10.1158/2767-9764.CRC-22-0433

27. Virani N, Kwon J, Zhou H, Mason R, Berbeco R, Protti A. *In vivo* hypoxia characterization using blood oxygen level dependent magnetic resonance imaging in a preclinical glioblastoma mouse model. *Magn Reson Imaging* (2021) 76(July 2020):52–60. doi: 10.1016/j.mri.2020.11.003

28. Toma-Dasu I, Uhrdin J, Antonovic L, Dasu A, Nuyts S, Dirix P, et al. Dose prescription and treatment planning based on FMISO-PET hypoxia. *Acta Oncol (Madr)*. (2012) 51(2):222–30. doi: 10.3109/0284186X.2011.599815

29. Niyazi M, Andratschke N, Bendszus M, Chalmers AJ, Erridge SC, Galdiks N, et al. ESTRO-EANO guideline on target delineation and radiotherapy details for glioblastoma. *Radiother Oncol* (2023) 184:109663. doi: 10.1016/j.radonc.2023.109663

30. Wang GM, Cioffi G, Patil N, Waite KA, Lanese R, Ostrom QT, et al. Importance of the intersection of age and sex to understand variation in incidence and survival for primary Malignant gliomas. *Neuro Oncol* (2022) 24(2):302–10. doi: 10.1093/neuonc/noab199

31. Colopi A, Fuda S, Santi S, Onorato A, Cesarini V, Salvati M, et al. Impact of age and gender on glioblastoma onset, progression, and management. *Mech Ageing Dev* (2023) 211(January):111801. doi: 10.1016/j.mad.2023.111801

32. Tian M, Ma W, Chen Y, Yu Y, Zhu D, Shi J, et al. Impact of gender on the survival of patients with glioblastoma. *Biosci Rep* (2018) 38(6):1–9. doi: 10.1042/BSR20180752

33. Louis DN, Perry A, Wesseling P, Brat DJ, Cree IA, Figarella-branger D, et al. The 2021 WHO classification of tumors of the central nervous system: a summary. *Neuro Oncol* (2021) 23(June):1231–51. doi: 10.1093/neuonc/naab106

34. Stupp R, Mason WP, van den Bent MJ, Weller M, Fisher B, Taphoorn MJB, et al. Radiotherapy plus concomitant and adjuvant temozolomide for glioblastoma. *N Engl J Med* (2005) 352(10):987–96. doi: 10.1056/NEJMoa043330

35. Chakhoyan A, Guillamo J-S, Collet S, Kauffmann F, Delcroix N, Lechapt-Zalcman E, et al. FMISO-PET-derived brain oxygen tension maps: application to glioblastoma and less aggressive gliomas. *Sci Rep* (2017) 7(1):10210. doi: 10.1038/s41598-017-08646-y

36. O'Connor JPB, Robinson SP, Waterton JC. Imaging tumour hypoxia with oxygen-enhanced MRI and BOLD MRI. *Br J Radiol* (2019) 92(1096):20180642. doi: 10.1259/bjr.20180642

37. Tóth V, Förschler A, Hirsch NM, den Hollander J, Kooijman H, Gempt J, et al. MR-based hypoxia measures in human glioma. *J* (2013) 115(2):197–207. doi: 10.1007/s11060-013-1210-7

38. Fan Q, Tang CY, Gu D, Zhu J, Li G, Wu Y, et al. Investigation of hypoxia conditions using oxygen-enhanced magnetic resonance imaging measurements in glioma models. *Oncotarget* (2017) 8(19):31864–75. doi: 10.18632/oncotarget.16256

39. Linnik IV, Scott MLJ, Holliday KF, Woodhouse N, Waterton JC, O'Connor JPB, et al. Noninvasive tumor hypoxia measurement using magnetic resonance imaging in murine U87 glioma xenografts and in patients with glioblastoma. *Magn Reson Med* (2014) 71(5):1854–62. doi: 10.1002/mrm.24826

40. Tomppert A, Wuest W, Wiesmueller M, Heiss R, Kopp M, Nagel AM, et al. Achieving high spatial and temporal resolution with perfusion MRI in the head and neck region using golden-angle radial sampling. *Eur Radiol* (2021) 31(4):2263–71. doi: 10.1007/s00330-020-07263-0

41. O'Connor JPB, Boulton JKR, Jamin Y, Babur M, Finegan KG, Williams KJ, et al. Oxygen-enhanced MRI accurately identifies, quantifies, and maps tumor hypoxia in preclinical cancer models. *Cancer Res* (2016) 76(4):787–95. doi: 10.1158/0008-5472.CAN-15-2062

42. Keenan K, Boos M, Jackson EF, Kown S-J, Jennings D, Russek S. NIST/ISMRM MRI system phantom T1 measurements on multiple MRI system. *Proc 21th Sci Meet Int Soc Magn Reson Med* (2013) 21:4338.

43. Remmele S, Mason RP, O'Connor JPB. MRI hypoxia measurements. *Funct Imaging Oncology: Biophys Basis Tech Approaches* (2014) 1:269–89. doi: 10.1007/978-3-642-40412-2_12

44. Yang DM, Arai TJ, Campbell JW, Gerberich JL, Zhou H, Mason RP. Oxygen-sensitive MRI assessment of tumor response to hypoxic gas breathing challenge. *NMR Biomed* (2019) 32(7):e4101. doi: 10.1002/nbm.4101

45. Abdo R-A, Lamare F, Fernandez P, Bentourkia M. Analysis of hypoxia in human glioblastoma tumors with dynamic 18F-FMISO PET imaging. *Australas Phys Eng Sci Med [Internet]*. (2019) 42(4):981–93. doi: 10.1007/s13246-019-00797-8

46. Hanspach J, Nagel AM, Hensel B, Uder M, Koros L, Laun FB. Sample size estimation: Current practice and considerations for original investigations in MRI technical development studies. *Magn Reson Med* (2021) 85(4):2109–16. doi: 10.1002/mrm.28550

47. Danzer MF, Eveslage M, Görlich D, Noto B. A statistical framework for planning and analysing test-retest studies for repeatability of quantitative biomarker measurements. *arXiv e-prints* (2023), arXiv:2301. doi: 10.48550/arXiv.2301.11690

48. Dubec MJ, Buckley DL, Berks M, Clough A, Gaffney J, Datta A, et al. First-in-human technique translation of oxygen-enhanced MRI to an MR linac system in patients with head and neck cancer. *Radiother Oncol* (2023) 183:109592. doi: 10.1016/j.radonc.2023.109592